AIAA JOURNAL
Vol. 35, No. 3, March 1997

Evaluation of Data Reduction Methods for the Mixed Mode Bending Test

Srinivas Bhashyam* and Barry D. Davidson†
Syracuse University, Syracuse, New York 13244-1240

Results are presented from a combined numerical and experimental study to assess the accuracy of six different methods of data reduction for the mixed-mode bending test. These include two methods in the literature that use only the load data from the test, a modification to one of these methods to improve accuracy, two variations of compliance calibration, and a newly proposed "load-deflection method." First, the accuracy of the various methods were evaluated by comparison to finite element predictions for a typical laminate. Second, the various methods were applied to double cantilever beam and end-notched flexure test data that had previously been reduced by well-established techniques. Finally, five laminates were tested in the mixed-mode bending fixture at each of five mode ratios: $G_{II}/G = 0.2, 0.4, 0.6, 0.8$, and 1.0. The data from these tests were reduced by the various data reduction methods. The mean value of the critical energy release rate G_c at $G_{II}/G = 0.4$ was compared to the mean G_c obtained by compliance calibration of a separate set of five single leg bending test specimens, and G_c at $G_{II}/G = 1.0$ was compared to the mean G_c obtained by compliance calibration of a separate set of five end-notched flexure test specimens. By these comparisons, by physical considerations of the test results, and by examinations of the standard deviations of the various data pools, it was concluded that a method that uses only load data from the test is the most accurate. For improved accuracy, a modification to this method is suggested that involves only the experimental determination of the bending rigidities of the cracked and uncracked regions and the use of these results in the reduction of data.

Introduction

DELAMINATION is a primary mode of failure in laminated composite materials. To predict delamination growth, the energy available to create a unit of new surface area through delamination, referred to as the energy release rate G, can first be calculated through analytical or numerical techniques. This value can then be compared to the critical energy release rate G_c, also called the delamination toughness of the material. The delamination toughness of laminated composites under pure mode I and pure mode II loading can be determined experimentally through the double cantilever beam (DCB) test[1] and the end-notched flexure (ENF) test,[2] respectively. In practical structures, however, delamination growth generally occurs under the combined influence of mode I and mode II loading. Hence, it is important to determine the mixed-mode I/II delamination toughness of the material of interest.

There are a number of mixed-mode test methods that have been used for laminated composites (see, for example, the review in Ref. 3). Of these, the mixed-mode bending (MMB) test[3,4] has perhaps found the most widespread usage. Most likely, this is because the MMB test may be used with a single type of test specimen to produce fracture under a complete range of mixed-mode I/II conditions. The MMB test essentially combines the DCB and the ENF loadings into a single test. Schematic diagrams of the test apparatus and the test specimen are shown in Fig. 1. By applying a load P through a loading lever as shown, mode I, mode II, or combined conditions may be produced at the crack tip. The position of the loading lever, denoted as c in Fig. 1a, determines the mode ratio for the test. Pure mode I loading results when the loading lever is removed and an upward load is applied to the hinge. Pure mode II loading results when the load is applied such that $c \leq L/3$. Any other position produces mixed-mode loading conditions. In Fig. 1a, W_L is the weight of the lever arm, F_s is the spring force from the displacement transducer, which is newly introduced here, and c_g is the distance from the center of gravity of the loading lever to the center pin. As will be described later, the displacement transducer is used to measure the opening deflection between the cracked regions of the specimen.

Several data reduction methods are currently being used to obtain G_c from MMB test data. These include 1) the method of Reeder and Crews,[3,4] 2) the method of Kinloch et al.,[5] and 3) the compliance calibration method.[6,7] In addition to these existing methods, a load-deflection method has recently been proposed[8] and is described in this work. A modification to the method of Kinloch et al.[5] that will result in increased accuracy is also described and is referred to herein as the modified Kinloch method. It is not clear, however, which of these data reduction methods will result in the most accurate values of G_c. Thus, all of the cited data reduction methods are evaluated for accuracy and ease of use.

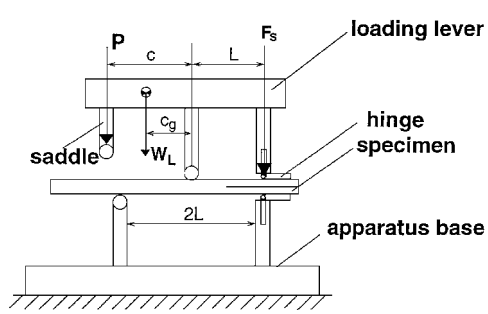

a) Schematic diagram of the MMB test fixture

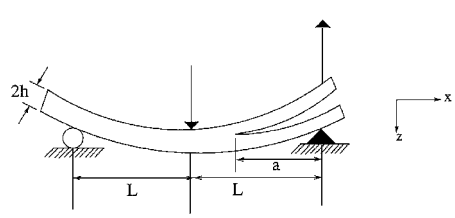

b) Test specimen and loading

Fig. 1 Mixed-mode bending test.

Received Feb. 21, 1996; revision received Oct. 15, 1996; accepted for publication Nov. 10, 1996; also published in *AIAA Journal on Disc*, Volume 2, Number 2.

*Graduate Research Assistant, Department of Mechanical, Aerospace, and Manufacturing Engineering.

†Associate Professor, Department of Mechanical, Aerospace, and Manufacturing Engineering.

Data Reduction Methods

Method of Reeder and Crews

Reeder and Crews[3,4] have employed a modified beam theory approach to determine the mode I and mode II energy release rates using closed-form expressions. In their work, the MMB test was represented as a superposition of mode I and mode II loadings. This superposition analysis allows a direct separation of the mode I and mode II components of loading, P_I and P_{II}, respectively. Taking into account the weight of the lever arm W_L and the spring force F_s from the displacement transducer, the equations for P_I and P_{II} are given by a minor modification of the expressions given by Reeder[9] as

$$P_I = P\left(\frac{3c - L}{4L}\right) + W_L\left(\frac{3c_g - L}{4L}\right) - F_s \tag{1}$$

$$P_{II} = P[(c + L)/L] + W_L[(c_g + L)/L] \tag{2}$$

where P is the total applied load and L is the half-span length (Fig. 1). The expression for the mode I and mode II energy release rates, G_I and G_{II}, respectively, are obtained from modified beam theory and are given by[3]

$$G_I = \frac{12P_I^2}{B^2h^3E_{11}}\left(a^2 + \frac{2a}{\lambda} + \frac{1}{\lambda^2} + \frac{h^2E_{11}}{10G_{13}}\right) \tag{3}$$

$$G_{II} = \frac{9P_{II}^2}{16B^2h^3E_{11}}\left(a^2 + \frac{0.2h^2E_{11}}{G_{13}}\right) \tag{4}$$

where

$$\lambda = \left(\frac{6E_{33}}{h^4E_{11}}\right)^{\frac{1}{4}} \tag{5}$$

Here, E_{11} is the elastic modulus of the specimen in the x direction, E_{33} is the elastic modulus of the specimen in the z direction, G_{13} is the specimen's shear modulus in the x–z plane, h is one-half the specimen's thickness in the uncracked region (Fig. 1), and B is the specimen's width. The total energy release rate is given by

$$G = G_I + G_{II} \tag{6}$$

The method of Reeder and Crews[3,4] will be subsequently referred to as the RC method.

Original Method of Kinloch et al.

Kinloch et al.[5] also used a beam theory approach to obtain G_I and G_{II}. However, in their approach, an effective crack length is used to account for the contribution to the energy release rate from shear deformations. A modified version of the expressions presented in Ref. 5 for a unidirectional specimen subjected to the MMB loading yields

$$G_I = \frac{12P_I^2(a + \chi h)^2}{B^2E_{11}^fh^3} \tag{7}$$

$$G_{II} = \frac{9P_{II}^2(a + 0.42\chi h)^2}{16B^2E_{11}^fh^3} \tag{8}$$

where E_{11}^f is the flexural modulus in the x direction and P_I and P_{II} are given by Eqs. (1) and (2), respectively. Equations (7) and (8) differ from those in Ref. 5 only in that the flexural modulus E_{11}^f is used in place of the longitudinal modulus E_{11}. The correction factor χ used to obtain an effective crack length in Eqs. (7) and (8) is defined as

$$\chi = \sqrt{\frac{E_{11}^f}{11G_{13}}}\left[3 - 2\left(\frac{\Gamma}{\Gamma + 1}\right)^2\right]^{\frac{1}{2}} \tag{9}$$

where

$$\Gamma = 1.18\frac{(E_{11}^fE_{33})^{\frac{1}{2}}}{G_{13}} \tag{10}$$

We examined the experimental method[10] of determining χ using DCB data and found that there was a large specimen-to-specimen variation in its value.[8] Because χ cannot be determined for each and every MMB specimen that is tested, it was concluded that the only viable option was to use the preceding analytical expressions. Reference 5 also presents corrections to the energy release rate expressions to account for large lever arm rotations and large deflections of the cracked regions of the specimen. These effects may be important in testing very tough composites, such as those with thermoplastic matrices. For all data reported herein, these corrections were evaluated and were found to change G_c by a negligible amount[8] and are therefore not included when presenting results. The original method of Kinloch et al., as just outlined, will be referred to subsequently as the OK method.

Modified Kinloch Method

The previous two data reduction methods implicitly assume that the ratio of bending rigidities of the uncracked and cracked regions is 8/1. This is true for a homogeneous material. However, nonuniform fiber distributions and the effect of finite roller diameter generally causes the experimentally observed ratio of bending rigidities to differ from this theoretical result.[11]

In the modified Kinloch or MK method, the equations for energy release rates are recast in terms of the bending rigidities of the specimen. The resulting equations for G_I and G_{II} are[8,11,12]

$$G_I = \frac{P_I^2(a + \chi h)^2}{B^2D_1} \tag{11}$$

$$G_{II} = \frac{(R - 2)P_{II}^2(a + 0.42\chi h)^2}{16B^2D} \tag{12}$$

In these equations, D is the bending rigidity of the uncracked region of the specimen, D_1 is the bending rigidity of the cracked region, and R is their ratio, i.e., $R = D/D_1$. Note that for a unidirectional specimen with a homogeneous through-the-thickness fiber distribution in plane stress, Eqs. (11) and (12) reduce to Eqs. (7) and (8), and E_{11}^f can be replaced by E_{11}. In the MK method, the values of D, D_1, and R are experimentally determined using three-point-bending tests. Note that if E_{11}^f is determined experimentally for use with the OK method, then the only difference between the OK method and the MK method is the assumption of $R = 8$ in the former case.

Compliance Calibration Method

The compliance calibration (CC) method works on the fundamental principle that, for a linear elastic specimen that contains a crack and that is loaded at a single point, the energy release rate is given by[13]

$$G = \frac{P^2}{2B}\frac{\partial C}{\partial a} \tag{13}$$

Here, P is the applied load, C is the specimen's compliance, and a is the crack length. This is a well-established data reduction procedure for the DCB and ENF tests.[1,11,14,15] The CC method has also been recently proposed[6,7] for use with the MMB test. It has been assumed that the CC method works for the MMB test if it is possible to separate out the mode I and mode II components of deflections, δ_I and δ_{II}, respectively, along with the mode I and mode II components of load, P_I and P_{II}. Then, the mode I and mode II compliances, C_I and C_{II}, respectively, can be expressed as

$$C_I = \delta_I/P_I; \qquad C_{II} = \delta_{II}/P_{II} \tag{14}$$

The mode I and mode II compliances can be determined experimentally as a function of crack length during the test. Curve fits are then used to obtain equations for C_I and C_{II} as a function of crack length, and the individual energy release rate components, G_I and G_{II}, are obtained by substituting these expressions, along with P_I and P_{II}, into Eq. (13). The critical energy release rate components as a function of crack length may be determined by evaluating the derivatives at the various crack lengths where crack advance occurred. Note that, for this method to work, crack growth must be stable. For the MMB test under the conventional actuator displacement control, stable crack advance occurs only for certain mode

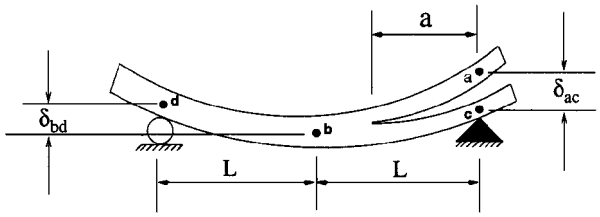

Fig. 2 Deformations of the MMB specimen.

ratios, which are dependent on the crack length.[3] However, it has been shown[7] that by controlling the test machine off of the crack opening displacement, stable crack advance is obtained at all mode ratios except pure mode II.

Figure 2 shows the deformation of the MMB test specimen. In this figure, δ_{ac} is the opening deflection between the cracked regions and δ_{bd} is the specimen's center-point deflection. Points a and c represent the midplane of the upper and lower cracked regions of the specimen above the support point, respectively, and points b and d represent the midplane of the uncracked region of the specimen at the point of load application and at the left support, respectively. A deflection superposition analysis has been carried out to separate the mode I and mode II components of deflection, and the resulting expressions for the case of small deflections are[8]

$$\delta_I = \delta_{ac}; \qquad \delta_{II} = \delta_{bd} + (\delta_I/4) \tag{15}$$

These expressions for the mode I and mode II deflections are identical to those given in Refs. 6 and 7. In our test setup, the opening deflection δ_{ac} is measured using a linear variable displacement transducer (LVDT), which is also used to control the test machine. The specimen's center-point deflection δ_{bd} is measured directly using a dial gauge. Using the MMB test results reported subsequently, we compared the direct measurement of the center-point deflection with the procedure used in Ref. 7, where this value was deduced from δ_{ac} and from the test machine's actuator displacement. It was found that the method of Ref. 7 consistently gave larger deflections, on the order of 0.5 mm, than was observed in the dial gauge. This was attributed to the play in the pins and bearings and connections of the MMB fixture. This would likely generally be the case, unless all components of the system were manufactured with extremely tight tolerances. As such, the method of Ref. 7 is not considered highly reliable. This is particularly important as small changes in compliance can produce large changes in dC/da.

The curve fit used in this work for the mode I compliance C_I is the same as that used for the DCB and is given by[1]

$$C_I = ma^n \tag{16}$$

In Ref. 7, a modified power law of the form

$$C_I = m(a + \chi h)^3 \tag{17}$$

is used to fit the mode I compliance data.

Several variations of a cubic polynomial can be used to fit the mode II compliance. The first form is the full cubic polynomial that has been used for the ENF test[11,14]

$$C_{II} = C_0 + C_1 a + C_2 a^2 + C_3 a^3 \tag{18}$$

ENF test data have also been fit with the second-order term removed,[15] i.e.,

$$C_{II} = C_0 + C_1 a + C_3 a^3 \tag{19}$$

This polynomial was found to be superior to Eq. (18) for fitting MMB test data,[8] as it often eliminates inflection points in the compliance vs crack length curve. The third form for the mode II compliance is that used in Ref. 7 for the MMB, and also evaluated in Refs. 11 and 15 for the ENF,

$$C_{II} = C_0 + C_3 a^3 \tag{20}$$

The curve fits given by both Eqs. (19) and (20) will be examined. When Eq. (19) is used, this method will be referred to as CC1, and when Eq. (20) is used we will refer to this method as CC2.

Load-Deflection Method

The RC method, the OK method, and the MK method all show a dependence on material properties, and it may be preferable to use a data reduction method that is material property independent. One such method presented in the preceding section was CC for use with the MMB. Next, a second method, referred to as the load-deflection (LD) method,[8] is described.

The LD method uses both the load and deflection data from the MMB test to determine the individual energy release rate components. Because, in the MMB test, loads as well as deflections can be separated into their mode I and mode II components, the expression for mode I energy release rate is the same as that for the DCB and is given by[10]

$$G_I = \frac{3P_I\delta_I}{2B(a + \chi h)} \tag{21}$$

To obtain the mode II component, compare Eqs. (12) and (13) to determine dC_{II}/da, integrate this result to obtain C_{II}, and substitute the result back into Eq. (12) to obtain

$$G_{II} = \frac{3P_{II}\delta_{II}(R-2)(a + 0.42\chi h)^2}{2B[4L^3 + (R-2)(a + 0.42\chi h)^3]} \tag{22}$$

These equations have only a weak dependence on material properties through χ and, for G_{II} only, through R.

Preliminary Evaluation of Methods

Comparison with Finite Element Results

As an initial evaluation of accuracy, results for G_I and G_{II} as obtained by all of the data reduction methods, with the exception of the MK method, were compared with finite element (FE) predictions. To this end, FE models were constructed for MMB loadings that created mode ratios G_{II}/G of approximately 0.2, 0.4, 0.6, 0.8, and 1.0. All models considered a $[0]_{24}$ laminate with a midplane delamination, a crack length a of 25.4 mm, and a half-span length L of 50.8 mm. Material properties were taken to be those for Ciba Giegy C12K/R6376 graphite/epoxy and were as given in the first two lines of Table 1, and E_{11}^f and E_{11} were taken to be equivalent. However, for these calculations, a single-ply thickness of 0.127 mm was used.[11,14] Thus, the half-thicknesses h of the laminates that were modeled were 1.52 mm. The models used eight-noded plane stress isoparametric elements and were constructed and analyzed using the commercially available FE code ABAQUS, licensed from Hibbitt, Karlsson, and Sorensen, Inc. Energy release rates as predicted by the FE method were obtained by the virtual crack closure technique,[16] which was assumed to be the most accurate of all methods. Mesh refinement studies were performed to ascertain the independence of the FE results with respect to the meshing technique.[8]

Table 2 presents the results of this preliminary study. In all cases, the total applied load P was taken equal to 1 N and the specimen's width B was taken equal to 1 mm. Also, the weight of the lever arm W_L and the spring force F_s were neglected. With these modifications, the mode I and mode II load components were determined from Eqs. (1) and (2). No lever arm was included in the model; rather, the loads P_I and P_{II} were applied directly to the FE model of the specimen. For the RC method, energy release rates were computed from Eqs. (3) and (4), and for the OK method they were computed from Eqs. (7) and (8). The values of the opening deflection δ_{ac} and the specimen's center-point deflection δ_{bd} (Fig. 2) were obtained from the FE output and were used in Eqs. (15), (21), and (22) to compute the energy release rates for the LD method. For the CC methods, additional FE models were constructed with various crack lengths up to a maximum of $a = 38.1$ mm. The mode I and mode II components of deflection were computed identically as was done for

Table 1 Material and structural properties for a $[0]_{24}$ Ciba–Giegy C12K/R6376 laminate

$E_{11} = 146.86$ GPa; $E_{22} = E_{33} = 10.62$ GPa; $\nu_{12} = 0.33$
$G_{12} = G_{13} = 5.45$ GPa; $\chi = 1.85$
$E_{11}^f = 114.15$ GPa; $D = 485.12$ Nm; $D_1 = 66.30$ Nm; $R = 7.317$
Single ply thickness $= 1.545 \times 10^{-4}$ m

Table 2 Comparison of energy release rates (joules per square meter) with FE predictions

G_{II}/G		FE	RC	% Error	OK	% Error	LD	% Error	CC1	% Error	CC2	% Error
0.2	G_I	25.74	24.29	−5.61	25.79	0.17	25.89	0.58	26.26	2.02	26.26	2.02
	G_{II}	6.52	6.08	−6.88	6.53	0.07	6.67	2.30	6.53	0.15	6.35	−2.61
	G	32.26	30.37	−5.87	32.32	0.15	32.56	0.90	32.79	1.64	32.61	1.05
0.4	G_I	4.56	4.31	−5.61	4.57	0.17	4.59	0.66	4.76	4.32	4.76	4.32
	G_{II}	3.09	2.87	−6.87	3.08	−0.08	3.16	2.27	3.11	0.49	3.02	−2.20
	G	7.65	7.18	−6.12	7.65	0.05	7.75	1.44	7.87	3.01	7.78	1.82
0.6	G_I	1.48	1.40	−5.65	1.49	0.17	1.49	0.17	1.52	2.64	1.52	2.64
	G_{II}	2.26	2.11	−6.87	2.27	0.09	2.31	2.21	2.28	0.84	2.21	−2.26
	G	3.74	3.51	−6.39	3.76	0.05	3.80	1.33	3.80	1.33	3.73	−0.59
0.8	G_I	0.45	0.42	−6.42	0.44	−0.73	0.45	0.22	0.46	1.56	0.46	1.56
	G_{II}	1.85	1.72	−7.00	1.84	−0.07	1.88	1.62	1.84	−0.54	1.79	−3.14
	G	2.30	2.14	−6.88	2.30	−0.26	2.34	1.74	2.28	0.00	2.25	−2.17
1.0	G_{II}	1.38	1.29	−6.88	1.37	−0.01	1.41	2.17	1.38	0.00	1.34	−2.89

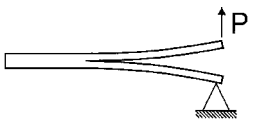

Fig. 3a Double cantilever beam test.

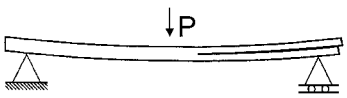

Fig. 3b End-notched flexure test.

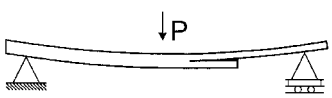

Fig. 3c Single-leg-bending test.

the LD method. These values were used to obtain mode I and mode II compliances from Eq. (14). The mode I compliance as a function of crack length was fit with the power law of Eq. (16). For CC1, the mode II compliance as a function of crack length data was fit using Eq. (19), whereas for CC2, Eq. (20) was used. Equation (13), along with the appropriate derivative and load component, was used to obtain G_I and G_{II}. Initially, the curve fits were based on compliance results from five specimens with crack lengths of 25.40, 27.94, 30.48, 33.02, and 35.56 mm. Subsequent evaluations of curve fits obtained by keeping the first crack length the same, but by varying the other crack lengths, produced no appreciable change in results.

From Table 2, it can be seen that the OK method exhibits the closest agreement with the FE results, whereas the RC method shows the largest discrepancies. The LD, CC1, and CC2 methods are all very good and roughly equivalent. The CC1 and CC2 methods only differ in their mode II components, and as might be expected, the CC1 method is observed to be slightly more accurate for G_{II}. The results for CC1 and CC2 in the table clearly show the potential applicability of the CC method to the MMB test. Finally, we point out that a similar FE study, which evaluated only pure mode II loadings and only the OK and RC methods, found better correlation for the OK than the RC method.[17]

Comparison to DCB and ENF Compliance Calibration Results

As a secondary evaluation of the accuracy of the various data reduction methods, determinations of G_{Ic} and G_{IIc} by the RC, OK, and LD methods were compared to CC results for 10 different DCB specimens and 15 different ENF specimens. These tests were performed at Syracuse University, and a subset of these results have been presented in Ref. 14.

Schematic diagrams of the DCB and ENF tests are shown in Figs. 3a and 3b, respectively. In the DCB test,[1] a vertical load is applied at the tip of one of the cracked regions of a symmetrically cracked specimen, and the tip of the other cracked region is held fixed. Because crack growth is stable under displacement control, it is possible to obtain compliance values at several crack lengths where crack advance occurs. In our tests, a curve fit of the form given by Eq. (16) was used to fit the compliance as a function of crack length data. The derivative of the compliance at the initial crack length where the crack advanced, from a 12.7-μm thick Teflon® insert, was used along with the corresponding critical load and Eq. (13) to obtain a nonprecracked value of G_{Ic}. To obtain a precracked G_{Ic}, the derivative of compliance, the critical load, and Eq. (13) were all evaluated at the crack length where the next increment of crack advance occurred. This CC data reduction procedure for the DCB test results in highly accurate values of G_{Ic}. Additional details are provided in Ref. 14.

In the ENF test,[2] a load is applied at the center point of a symmetrically cracked specimen, as shown in Fig. 3b. Unlike the DCB, crack growth is unstable in the ENF. Thus, the CC procedure is different. Compliance data are obtained by first placing the specimen appropriately in the test fixture to obtain various crack lengths and then loading it to approximately 50% of the critical load.[14] The compliance is found from the slope of a linear least-squares curve fit of the deflection vs load data. Different crack lengths are obtained by sliding the specimen in the test fixture. The crack lengths are chosen such that the crack length at which the fracture test will be performed is the median value. In our work, a cubic polynomial of the form given by Eq. (18) was used to fit the compliance as a function of crack length data. The derivative of the compliance at the crack length where the specimen is to be fractured, along with the critical load from the fracture test itself, was used to calculate a nonprecracked value of G_{IIc}. To obtain a precracked G_{IIc}, different specimens were precracked in mode II following the procedure described in Ref. 14. This CC procedure of data reduction for the ENF is considered to be the most accurate means of data reduction.[11, 12, 14, 15]

In the interests of brevity, the tabulated comparisons for the 35 specimens evaluated (10 nonprecracked DCB, 10 precracked DCB, 10 nonprecracked ENF, and 5 precracked ENF) are not presented here (full details are given in Ref. 8). Our conclusion from these comparisons was that somewhat better correlation to the CC results for all specimen and test types was obtained by the OK and LD methods than by the RC method.[8] In view of the better performance of the OK and the LD methods, as compared to the RC method, in our initial theoretical and experimental comparisons, the RC method was excluded from further study. The accuracies of the remaining data reduction techniques are evaluated in the next section.

Application of Methods to MMB

In this portion of the study, the relative accuracies of the OK, MK, LD, CC1, and CC2 methods of data reduction for the MMB test were evaluated experimentally. All experiments were conducted using 25-mm-wide, 24-ply, Ciba Giegy C12K/R6376 graphite/epoxy unidirectional specimens. All specimens contained a preimplanted 12.7-μm thick Teflon insert at their midplane. The material and structural properties for these specimens are given in Table 1. We point out that the single-ply thickness for the C12K/R6376 material used here is different from that used in Refs. 11 and 14. The material used here came from a different batch and contained a somewhat higher resin volume fraction. As such, it was found that the toughness of this batch was somewhat higher than that obtained for the material utilized in Refs. 11 and 14. Thus, the DCB, ENF, and single-leg-bending (SLB) test results that are reported in the following sections are different from those reported in our earlier works. These test results were obtained in a separate, companion study (also conducted at Syracuse University) to that described here.

MMB tests were run at mode ratios, G_{II}/G, of approximately 0.2, 0.4, 0.6, 0.8, and 1.0. All specimens had a crack length of 25.4 mm and a half-span length of 50.8 mm. All tests, except the pure mode II test, were run under opening displacement control. This was achieved by controlling the test machine directly from the LVDT that was used to measure the opening displacement δ_{ac}. As discussed previously, this control mode gives stable crack advance at all mode ratios except pure mode II. The mode II tests were run under actuator displacement control. Five specimens were tested at each mode ratio.

The data from all tests were reduced by all methods, except for the case of pure mode II where the CC method could not be used (due to unstable crack advance). The value of the critical load P_c from the test was transformed to its mode I and mode II components using Eqs. (1) and (2); the effect of lever arm weight W_L and LVDT spring force F_s were included in all calculations. For the OK method, Eqs. (7) and (8) were used for data reduction, where the flexural modulus was determined experimentally as the average of a series of three-point bending tests of the uncracked region of the plate from which the specimen was cut. For the MK method, Eqs. (11) and (12) were used for data reduction, where the flexural modulus of the cracked region was also determined experimentally as the average of a series of tests. To this end, all of the plates that were fabricated had a large piece of Teflon at one edge that provided a cracked region (half-laminate) that was approximately 25 $\times$ 150 mm. Typical structural properties used with the OK and MK methods are presented in the bottom portion of Table 1.

For data reduction by the LD, CC1, and CC2 methods, the opening deflection δ_{ac} was measured by an LVDT. To this end, our MMB fixture was modified, such that a cantilevered arm was attached to the fixture directly above the specimen's loading hinge. This arm extended out to the side of the specimen where it was contacted by the LVDT. The specimen's center-point deflection δ_{bd} was measured by a dial gauge. The values from the LVDT and dial gauge were transformed to the mode I and mode II components of deflection using Eq. (15). The LVDT deflections were obtained as a function of load from a companion data acquisition system. For the dial gauge deflections, a video camera was used to record the values of the center-point deflection during the test; a voltmeter correlated to load was also placed in this video image. After the test, the video was played back to obtain the deflection at the instant of fracture for the LD method, or the deflection as a function of load for the CC1 and CC2 methods. The critical values of the mode I and mode II deflections, as given by Eq. (15), along with the critical loads, were used to determine G_{Ic} and G_{IIc} in the LD method. For the CC methods, the compliance as a function of crack length data was determined for a minimum of five increments of crack advance. In all cases, the first two specimens tested at each mode ratio were unloaded fully at each increment of crack advance. After each increment, the crack length on either side of the specimen was measured with a traveling microscope, and the average of these two values was used for subsequent data reduction. The compliance was then determined by a linear regression analysis of the mode I displacement vs mode I load data and of the mode II displacement vs mode II load data [cf. Eqs. (1), (2), (14), and (15)]. In all cases, this was found to correlate well with the compliance obtained by simply taking the critical mode I or mode II displacement and dividing by the appropriate (mode I or mode II) load. Thus, for the remaining three specimens, the compliance as a function of crack length was obtained by this latter, simpler method. For both the CC1 and CC2 methods, Eq. (16) was used to fit the mode I compliance data. For the CC1 method, Eq. (19) was used to fit the mode II compliance data, and for the CC2 method, Eq. (20) was used.

All data reduction methods were used to obtain nonprecracked and precracked toughness data. The nonprecracked G_c was defined to be that value obtained from the increment of crack advance that initiated directly from the Teflon insert, and the precracked G_c was obtained from the next increment of crack advance.

Comparison Standards

Critical energy release rates as obtained from DCB, ENF, and SLB tests were used as comparison standards by which the accuracy of the various data reduction methods were assessed. These tests were run on unidirectional laminates from the same batch of material in a companion study. The data from all three tests were reduced by CC and as such are considered highly accurate. For each test, five specimens were tested in the nonprecracked condition (i.e., directly from the 12.7-μm Teflon insert), and except for ENF, five were tested in a precracked condition. Details of these tests were identical to those described in Ref. 14, although, as already described, the results of this reference were not used for comparison due to batch-to-batch variation. As will become apparent, the primary comparison standard is the SLB test. This test is pictured in Fig. 3c. For a specimen with a midplane delamination, this test produces a mode ratio G_{II}/G equal to 0.4 (Ref. 14) and is conducted essentially the same as the ENF test. The compliance of the specimen as a function of crack length is determined prior to the fracture test by appropriately placing the specimen in the fixture. Because of the fact that crack advance is not occurring during the CC test for the SLB, the crack length is very accurately known, the crack front is straight, and highly accurate results are obtained. In addition, similar to the ENF, because Eq. (13) is applied at a crack length at the median of the experimentally determined compliance vs crack length results, error associated with numerically differentiating data near the beginning or end of a curve is avoided. This issue is discussed in more detail in a subsequent section.

Results and Discussion

The values of G_c as obtained from all of the data reduction methods are shown graphically in the fracture interaction diagrams of Figs. 4 and 5. Figure 4 presents results for the nonprecracked specimens, whereas Fig. 5 presents results for the precracked specimens. On the same graphs, the CC values of G_c that were obtained from the DCB, SLB, and ENF tests are also shown. Each point in the figures represents, for a given data reduction method, the average critical energy release rate of the five tests, plotted on the vertical axis, and the average mode ratio of the five tests plotted on the horizontal axis. That is, each individual MMB specimen had a slightly different mode ratio, and the actual test results would appear as a small cloud surrounding the average. In the interests of clarity, only the averages are shown here.

Initially, we focus attention on the calibration standard of the SLB test at a mode ratio of 0.4. Both the nonprecracked and precracked results indicate that the MK method is nearest the calibration

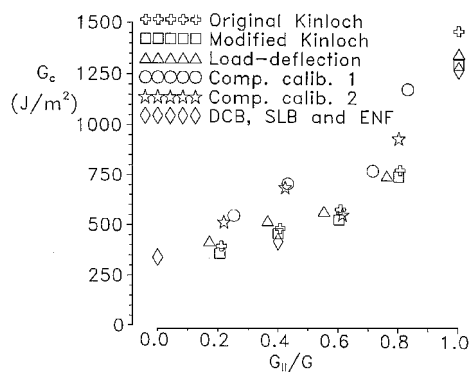

Fig. 4 Nonprecracked fracture interaction diagram.

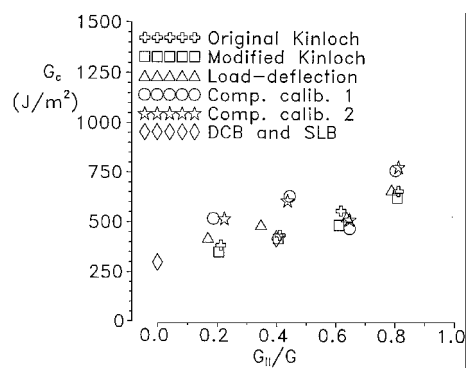

Fig. 5 Precracked fracture interaction diagram.

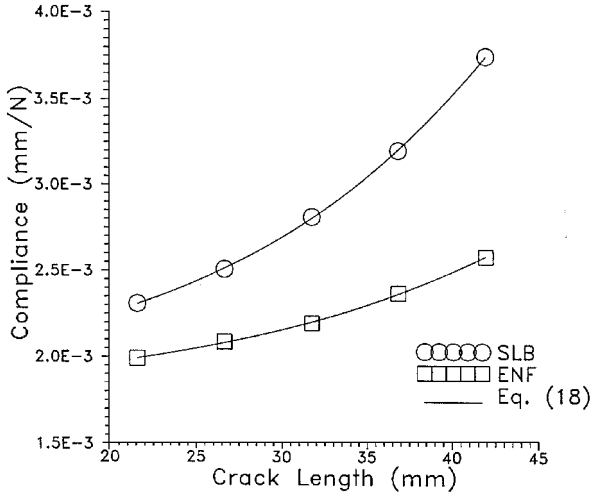

Fig. 6 Compliance calibration results for SLB and ENF specimens.

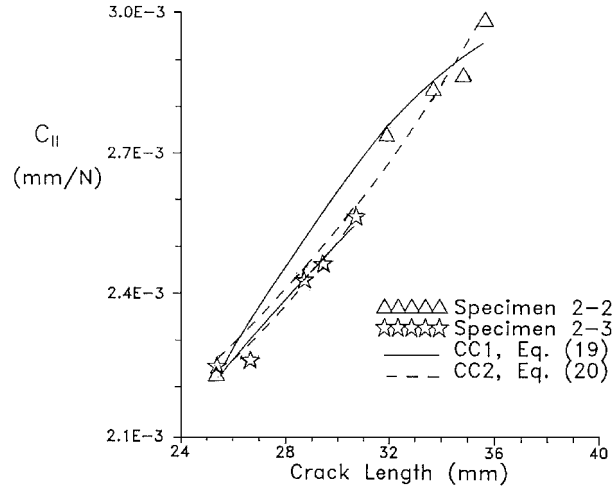

Fig. 7 Mode II compliance results for MMB, $G_{II}/G = 0.4$.

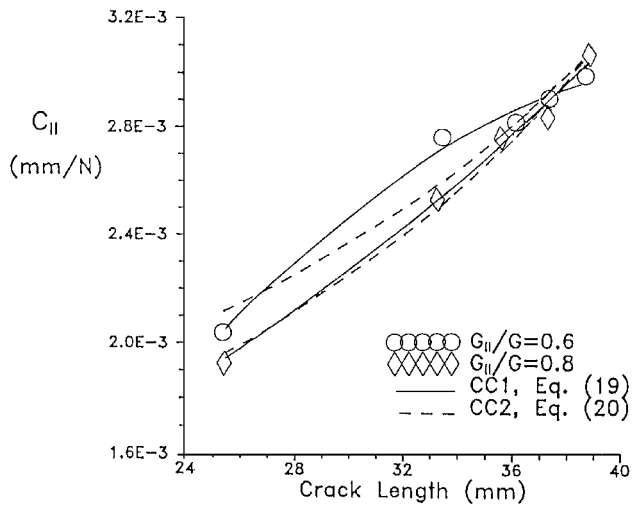

Fig. 8 Mode II compliance results for MMB.

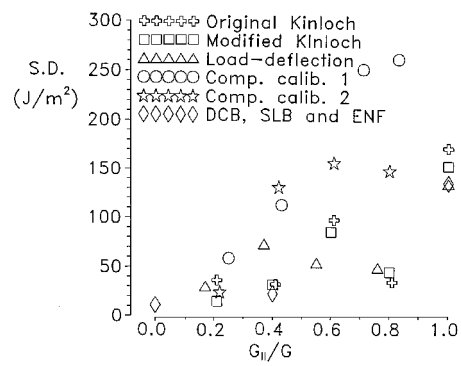

Fig. 9 Nonprecracked standard deviations.

standard, followed by the OK method and the LD method. It is difficult to state categorically that the MK method is best, because of the small sample sizes that were used. However, it is apparent from the data that these three methods are superior to the CC1 and CC2 methods. For later use, we point out here that the errors in the two CC methods were found to primarily be in their values for the mode II component of the critical energy release rate.

Next, consider the shape of the G_c vs mode mix curve. Physical considerations indicate that this curve should be reasonably smooth and, although not necessarily monotonically increasing, should likely not display the type of local minimum that is observed in the CC1 and CC2 data at a mode ratio near 0.6. In contrast, the shapes of the curves that are displayed by the MK, OK, and LD methods are physically reasonable and consistent. Finally, the good correlation of the MK, OK, and LD methods to the ENF nonprecracked results (Fig. 4) further corroborates their accuracies and lends an additional indication that the MK method is perhaps the best of the three.

Why do the CC1 and CC2 methods, which one may have initially expected to be best, produce poor results? For illustration, consider Fig. 6, which shows the CC results for typical SLB and ENF specimens. These data come from the calibration tests. The crack length at which the fracture tests were run was 31.75 mm; thus, CC was performed at two longer and two shorter crack lengths. The discrete symbols are the results of the compliance tests, and the solid curves are cubic polynomial curve fits of the form of Eq. (18). Notice that these curves are smooth and monotonically increasing without inflection points, and that all of the data points lie on the curve fit. This was typical of all of the SLB and ENF tests, and a repeat of these tests resulted in compliance curves that were essentially indistinguishable.[11,14] In addition, if all of the SLB compliance curves are presented on the same plot, or if all of the ENF curves are presented on the same plot, the spread in the data is found to be quite small.[11,14]

Contrast this to Figs. 7 and 8. Figure 7 presents typical mode II compliances as a function of crack length at a mode ratio of 0.4, and Fig. 8 presents similar data at mode ratios of 0.6 and 0.8. These specific specimens were chosen as they were closest to the mean of the CC1 and CC2 results at their respective mode ratios; thus, they are neither best case nor worst case. Observe that the assumed forms of the compliance curves, be it Eq. (19) or (20), are only able to simulate the trends of the data in a relatively broad sense. That is, the experimentally determined mode II component of compliance values do not generally follow the assumed functional forms, and dC_{II}/da as obtained numerically is therefore not necessarily reflective of the actual behavior of the specimen. Also note that the specimen-to-specimen variation in dC_{II}/da is large and was found to be significantly more than that observed for ENF specimens.[11] The inability of the assumed form of the compliance curve to fit the data for any individual specimen results in large errors in the CC1 and CC2 data, as well as large specimen-to-specimen variations. This is further evidenced by Figs. 9 and 10, which present the normal standard deviations of the nonprecracked and precracked toughness data, respectively, which were presented in Figs. 4 and 5. For the most part, the standard deviations of the CC1 and CC2 data are much larger than those observed from the other data reduction methods, and therefore corroborate the trends already described. It is likely that the large errors in the CC methods for the MMB test occur primarily due to nonstraight and nonuniform crack advance. That is, small changes in the length of the crack at either edge, and therefore in the crack front shape, likely have a large effect on compliance (fiber bridging may also be a consideration; however, this phenomenon was not evidenced by our material[14]). It follows that at any given crack length one could artificially straighten the crack front and obtain a somewhat different CC curve. We checked the effect of this using the mode II compliance as a function of crack

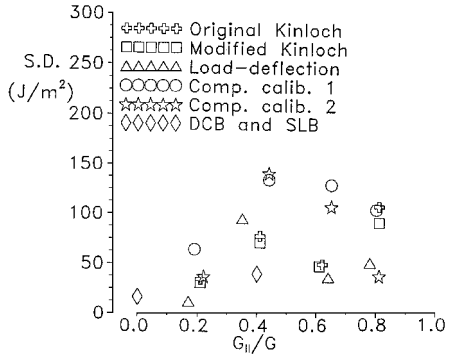

Fig. 10 Precracked standard deviations.

length results that were generated by the FE model. The value of compliance at a single crack length was perturbed by 2%, and the modified compliance results were then fit with an equation of the form of Eq. (19) or (20), and dC_{II}/da was determined. For CC1, it was found that dC_{II}/da at the first crack length could change by as much as 36% and at the second crack length could change by approximately 20%. For CC2, it was found that dC_{II}/da at the first crack length changed by as much as 5% and at the second crack length by approximately 3%. Larger changes are, of course, obtained when more than one compliance value is perturbed, or if the perturbation is larger than 2%. These results explain the better performance of CC2 as compared to CC1.

In contrast to this, it was found that the mode I component of the critical energy release rate as obtained from the CC1 and CC2 methods agreed reasonably closely with those obtained from the other methods (note that there is no difference in determining G_I by the two methods). A numerical study similar to that just described was also performed for this case. That is, the mode I component of compliance as a function of crack length results that were generated by the FE model were used to evaluate the effect on dC_I/da of perturbing one of the compliance values by a few percent. Following this perturbation, the resulting values of compliance as a function of crack length were fit with an equation of the form of Eq. (16). Little effect on dC_I/da was observed.

Conclusions

Results have been presented from a combined numerical and experimental evaluation of six different methods of data reduction for the mixed-mode bending test. These include methods or slight modifications to methods that are currently being used, as well as a newly proposed "load-deflection method." In terms of accuracy of the various methods when compared to numerical (FE) results, the original method of Kinloch et al. provided the best correlation. To account for uncertainties in material properties and nonhomogeneous distributions of the fibers throughout the laminate, a slight modification was suggested for practical use of this method. This modification involves only the experimental determination of the bending rigidities of the cracked and uncracked regions and the use of these results in the reduction of data. By comparison to SLB and ENF data, by physical considerations of the test results, and by examinations of the standard deviations of the various data pools, it was concluded that the modified Kinloch method provided the most accurate means of reducing the data from the MMB test to obtain critical energy release rates. The original method of Kinloch et al. will also produce accurate results, provided that an experimentally determined flexural modulus is utilized. When one of these approaches is adopted, it is best to experimentally determine the bending rigidities D and D_1 or the flexural modulus E_{11}^f from bending test specimens taken from each plate that is fabricated. These values may then be used for all specimens cut from that plate.

The MMB test is becoming a widely accepted method for characterizing the mixed-mode I/II delamination toughness of laminated composites. As has been done herein, it is not uncommon for the MMB test to be used, along with CC results from DCB and ENF tests, to develop a mode I/II fracture interaction diagram. It is our recommendation that the SLB test, with data reduction by CC, also be included as part of this procedure and that the data from the MMB test be reduced by the MK method. The SLB and ENF results may be used as a check of the accuracy of the data reduction procedure for the MMB. This eliminates any need for the complex setup required for the CC or LD methods of data reduction for the MMB test and, as has been demonstrated herein, results in a simple procedure with highly accurate results. It is pointed out that these conclusions only apply to unidirectional laminates with midplane delaminations, and it is likely that different conclusions would be reached if the MMB test were to be used for laminates with delaminations that were not at their midplane or for multidirectional layups.

Acknowledgment

This work was supported by the Federal Aviation Administration under Grant 94-G-022.

References

[1]Anon., "Standard Test Method for Mode I Interlaminar Fracture Toughness of Unidirectional Reinforced Polymer Matrix Composites, DCB Standard," ASTM Standard D5228-94, American Society of Testing and Materials, New York, 1994.

[2]Carlsson, L. A., Gillespie, J. W., and Pipes, R. B., "On the Analysis and Design of the End-Notched Flexure (ENF) Specimen for Mode II Testing," *Journal of Composite Materials*, Vol. 20, Nov. 1986, pp. 594–604.

[3]Reeder, J. R., and Crews, J. H., Jr., "The Mixed-Mode Bending Method for Delamination Testing," *AIAA Journal*, Vol. 28, No. 7, 1990, pp. 1270–1276.

[4]Reeder, J. R., and Crews, J. H., Jr., "Redesign of the Mixed-Mode Bending Delamination Test to Reduce Nonlinear Effects," *Journal of Composites Technology and Research*, Vol. 14, No. 1, 1992, pp. 12–19.

[5]Kinloch, A. J., Wang, Y., Williams, J. G., and Yayla, P., "The Mixed-Mode Delamination of Fiber Composite Materials," *Composites Science and Technology*, Vol. 47, No. 3, 1993, pp. 225–237.

[6]Thesken, J. C., Brandt, F., and Nilsson, S., "Investigation of Delamination Growth and Criticality Along Heterogeneous Interfaces," *Proceedings of the 19th Congress of the International Council of Aeronautical Sciences* (Anaheim, CA), 1994, pp. 995–1014.

[7]Martin, R. H., and Hansen, P. L., "Experimental Compliance Calibration for the MMB Specimen," *Composite Materials: Fatigue and Fracture—Sixth Volume*, edited by E. A. Armanios, American Society for Testing and Materials, New York (ASTM STP 1285) (to be published).

[8]Bhashyam, S., "An Evaluation of Data Reduction Methods for the Mixed-Mode Bending Test," M.S. Thesis, Dept. of Mechanical, Aerospace, and Manufacturing Engineering, Syracuse Univ., Syracuse, NY, May 1996.

[9]Reeder, J. R., "A Bilinear Failure Criterion for Mixed-Mode Delamination," *Composite Materials: Testing and Design (Eleventh Volume)*, edited by E. T. Camponeschi Jr., American Society of Testing and Materials, New York, 1993, pp. 303–322 (ASTM STP 1206).

[10]Williams, J. G., "The Fracture Mechanics of Delamination Tests," *Journal of Strain Analysis*, Vol. 24, No. 4, 1989, pp. 207–214.

[11]Davidson, B. D., Altonen, C. S., and Polaha, J. J., "Effect of Stacking Sequence on Delamination Toughness and Delamination Growth Behaviour in Composite End-Notched Flexure Specimens," *Composite Materials: Testing and Design (Twelfth Volume)*, edited by C. R. Saff and R. B. Deo, American Society for Testing and Materials, New York, 1996, pp. 393–413 (ASTM STP 1274).

[12]Davidson, B. D., Krüger, R., and König, M., "Three Dimensional Analysis and Resulting Design Recommendations for Unidirectional and Multidirectional End-Notched Flexure Tests," *Journal of Composite Materials*, Vol. 29, No. 3, 1995, pp. 2108–2133.

[13]Broek, D., *Elementary Engineering Fracture Mechanics*, Martinus–Nijhoff, Dordrecht, The Netherlands, 1982, pp. 123, 124.

[14]Polaha, J. J., Davidson, B. D., Hudson, R. C., and Pieracci, A., "Effects of Mode Ratio, Ply Orientation and Precracking on the Delamination Toughness of a Laminated Composite," *Journal of Reinforced Plastics and Composites*, Vol. 15, No. 2, 1996, pp. 141–173.

[15]O'Brien, T. K., Murri, G. B., and Salpekar, S. A., "Interlaminar Shear Fracture Toughness and Fatigue Thresholds for Composite Materials," *Composite Materials: Fatigue and Fracture—Second Volume*, edited by P. A. Lagace, American Society of Testing and Materials, New York, 1989, pp. 222–250 (ASTM STP 1012).

[16]Rybicki, E. F., and Kanninen, M. F., "A Finite Element Calculation of Stress Intensity Factors by a Modified Crack Closure Integral," *Engineering Fracture Mechanics*, Vol. 9, No. 4, 1977, pp. 931–938.

[17]Wang, Y., and Williams, J. G., "Correction Factors for Mode II Fracture Toughness Specimens of Composite Materials," *Composites Science and Technology*, Vol. 43, 1992, pp. 251–256.

G. Sutton
Editor-in-Chief